OsteoArthritis and Cartilage (2006) **14,** 571–579

doi:10.1016/j.joca.2005.12.003

Osteoarthritis and Cartilage

International Cartilage Repair Society

OARSI OSTEOARTHRITIS RESEARCH SOCIETY INTERNATIONAL

Viscoelastic properties of zonal articular chondrocytes measured by atomic force microscopy

E. M. Darling Ph.D.†‡§, S. Zauscher Ph.D.§‖ and F. Guilak Ph.D.†‡§‖*

† *Department of Surgery, Duke University Medical Center, Durham, NC 27710, USA*

‡ *Department of Biomedical Engineering, Duke University Medical Center, Durham, NC 27710, USA*

§ *Center for Biomolecular and Tissue Engineering, Duke University Medical Center, Durham, NC 27710, USA*

‖ *Department of Mechanical Engineering and Materials Science, Duke University Medical Center, Durham, NC 27710, USA*

Summary

Objective: Articular chondrocytes respond to chemical and mechanical signals depending on their zone of origin with respect to distance from the tissue surface. However, little is known of the zonal variations in cellular mechanical properties in cartilage. The goal of this study was to determine the zonal variations in the elastic and viscoelastic properties of porcine chondrocytes using atomic force microscopy (AFM), and to validate this method against micropipette aspiration.

Methods: A theoretical solution for stress relaxation of a viscoelastic, incompressible, isotropic surface indented with a hard, spherical indenter (5 μm diameter) was derived and fit to experimental stress-relaxation data for AFM indentation of chondrocytes isolated from the superficial or middle/deep zones of cartilage.

Results: The instantaneous moduli of chondrocytes were 0.55 ± 0.23 kPa for superficial cells (S) and 0.29 ± 0.14 kPa for middle/deep cells (M/D) ($P < 0.0001$), and the relaxed moduli were 0.31 ± 0.15 kPa (S) and 0.17 ± 0.09 kPa (M/D) ($P < 0.0001$). The apparent viscosities were 1.15 ± 0.66 kPa s (S) and 0.61 ± 0.69 kPa-s (M/D) ($P < 0.0001$). Results from the micropipette aspiration test showed similar cell moduli but higher apparent viscosities, indicating that mechanical properties measured by these two techniques are similar.

Conclusion: Our findings suggest that chondrocyte biomechanical properties differ significantly with the zone of origin, consistent with previous studies showing zonal differences in chondrocyte biosynthetic activity and gene expression. Given the versatility and dynamic testing capabilities of AFM, the ability to conduct stress-relaxation measurements using this technique may provide further insight into the viscoelastic properties of isolated cells.

Key words: Atomic force microscopy, Mechanotransduction, Stress relaxation, Scanning probe microscope, Osteoarthritis, Cell mechanics, Cytoskeleton.

Introduction

Articular cartilage is the connective tissue that lines the ends of bones in diarthrodial joints, providing a low-friction bearing surface for the transmission and distribution of mechanical loads in the skeleton. The tissue is maintained in a constant state of turnover through the anabolic and catabolic activities of the chondrocytes, the sole cell type in articular cartilage. As cartilage is avascular, alymphatic, and aneural, chondrocyte activity is believed to be regulated predominantly by local factors in the cellular microenvironment, including soluble mediators, matrix composition, and biophysical factors such as mechanical stress (reviewed in Refs. [1,2]). The response of chondrocytes to these factors depends on their site of origin in the tissue, and previous studies have shown significant differences in the phenotype, gene expression, and cytokine sensitivity of cells from the superficial zone of the tissue as compared to those from the middle/deep zones[3–11]. Furthermore, as the local mechanical environment of the cell is highly dependent on the relative properties of the cell, its pericellular matrix and the extracellular matrix in these regions[12], it would be expected that site-specific differences in these properties would significantly influence the cellular microenvironment[13]. While these variations have been studied in the pericellular matrix[13–15] and the extracellular matrix[16–18], little information is available on the site-specific differences in the mechanical properties of articular chondrocytes.

Several techniques have been used to determine the mechanical properties of single cells, including micropipette aspiration, compression within a gel matrix, unconfined compression, or various forms of cellular indentation, including cell poking, cytoindentation, or atomic force microscopy (AFM). Micropipette aspiration has been used extensively to study the biomechanical properties of articular chondrocytes[19–22]. In this procedure, a micropipette is placed at the cell wall and a negative pressure is applied, which deforms the cell membrane[23]. By analyzing the deformation and force response of the cell, elastic and

*Address correspondence and reprint requests to: Farshid Guilak, Ph.D., Orthopaedic Research Laboratories, 375 MSRB, Box 3093, Duke University Medical Center, Durham, NC 27710, USA. Tel: 1-919-684-2521; Fax: 1-919-681-8490; E-mail: guilak@duke.edu

Received 13 October 2005; revision accepted 13 December 2005.

viscoelastic properties can be determined[24,25]. An alternative method for monitoring the deformation behavior of single cells is to encapsulate them in a uniform matrix and apply an external strain[26,27]. To estimate cell stiffness, its deformation can be measured optically and compared to results obtained from theoretical models of the testing configuration. The "cell poker", another optical-based approach, was the first indentation-based technique for determining cellular mechanical properties that involves rapid indention of a cell[28–30]. "Cytoindentation" is a similar procedure but can be used to apply a variety of loading conditions[31,32]. Based on cantilever beam theory, the procedure involves indenting a cell with a small tip attached to a long cantilever. The amount of indentation is determined using laser light reflected off the cantilever and can be controlled so that creep indentation and stress-relaxation tests are possible. Unconfined compression is a recent variation on the cell indentation procedure, in which the tip size has been increased so that it is much larger than the cell. Using the same methodology, elastic and viscoelastic properties of single cells can be extracted[33].

AFM provides a high resolution form of the cell indentation procedure that enables measuring and imaging samples at the nanometer length scale[34–38]. This technique has been used previously to measure the mechanical properties of cartilaginous tissues[39–42], but only preliminary studies have been reported on its use to evaluate the properties of single chondrocytes[43–45]. Furthermore, few AFM studies have examined the viscoelastic properties of cells or tissues. One approach applied a dynamic loading profile to determine the frequency-dependent viscoelastic behavior of a biological material[46–48]. Standard viscoelastic tests, such as creep indentation and stress-relaxation, have been more difficult to implement using AFM due to control issues; however, new advances in AFM technology allow the programming of custom load or displacement profiles, which can be used to perform standard creep or stress-relaxation tests. To obtain intrinsic mechanical material properties, a mathematical model must be developed that accurately describes the testing configuration and must be based on an appropriate constitutive model[49].

The goal of this study was to develop a novel, AFM based stress-relaxation measurement approach to determine the viscoelastic properties of living cells and to test the hypothesis that the viscoelastic properties of chondrocytes vary with their zone of origin. Chondrocytes were isolated from the superficial or middle/deep zones of articular cartilage and tested using a novel stress-relaxation method to determine the instantaneous and equilibrium moduli and apparent viscosity of a cell based on a theoretical solution for small indentations of an isotropic, incompressible, viscoelastic surface with a hard, spherical indenter. Additionally, the viscoelastic properties of chondrocytes from the middle/deep zone were determined using a micropipette aspiration test, described previously[21], as a comparison to the AFM indentation method.

Materials and method

CHONDROCYTE HARVEST AND CULTURE CONDITIONS

Superficial and middle/deep zone articular chondrocytes were harvested from the femoral condyles of 2–3-year-old, skeletally mature pigs ($N = 8$) shortly after sacrifice. The superficial zone (~100 μm) was carefully removed from the surface of the cartilage using the zonal abrasion procedure[4]. After removing several more layers, the middle/deep zone (~500 μm) was harvested for subsequent digestion. Zonal tissues were placed in separate tubes of wash media containing high glucose Dulbecco's Modified Eagle Medium (DMEM) (Gibco, Carlsbad, CA), 1× gentamycin (Gibco), 1× kanamycin (Sigma, St. Louis, MO), and 1× fungizone (Gibco). Cells were released from their surrounding matrix using standard digestion techniques[50]. Briefly, the harvested tissue was incubated in 1% (wt/vol) pronase (Calbiochem, San Diego, CA) with 5% (wt/vol) fetal bovine serum (Gibco) for 1 h at 37 °C and 5% (vol/vol) CO_2.

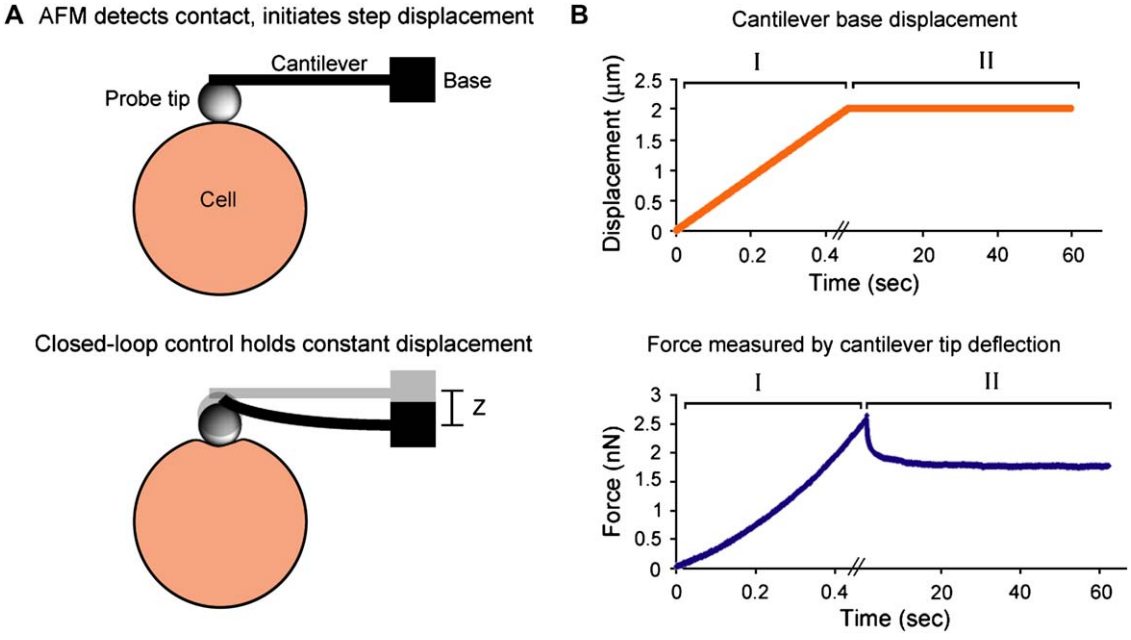

Fig. 1. Closed-loop control during stress-relaxation tests. A spherical probe indented the cell using an approximate step displacement, which was maintained by the AFM's closed-loop control software (A). Plots of the cantilever base movement and measured force visually described the elastic (B, Phase I) and viscoelastic (B, Phase II) responses of the cell.

Samples were then rinsed in wash media and placed in 0.4% (wt/vol) type II collagenase (Worthington, Lakewood, NJ) with 5% (wt/vol) fetal bovine serum for <2 h at 37°C and 5% CO_2. Following complete digestion, the cell solutions were centrifuged and rinsed in wash media. Final cell populations were resuspended in DMEM and seeded onto poly-L-lysine (PLL) coated slides (Wescor, Logan, UT). Chondrocytes placed on the PLL surface formed a strong attachment while retaining a rounded morphology. Biomechanical testing was performed at room temperature within 1–2 h of seeding.

ATOMIC FORCE MICROSCOPY

The biomechanical properties of superficial and middle/deep chondrocytes were measured using an atomic force microscope (MFP-3D, Asylum Research, Santa Barbara, CA). This instrument allows programming of custom force–displacement profiles, using the Igor Pro software (WaveMetrics, Inc., Portland, OR). Here we implemented closed-loop feedback control of the *z*-axis movement through a piezoelectric motor to maintain constant indentation displacement while conducting a stress-relaxation test on single cells (Fig. 1). To determine the indentation force applied to the cell, the deflection of the cantilever tip was measured optically from the position of a laser beam reflected off the cantilever tip onto a photosensitive detector. The applied force was determined by multiplying the cantilever stiffness by its deflection via Hooke's law ($F = kx$).

Gold-coated, 5 μm diameter, borosilicate, spherical tip cantilevers (Novascan Technologies, Inc., Ames, IA) were used for the AFM stress-relaxation experiments (Fig. 2). Cantilever spring constants (typically 0.065 N/m) were determined from the power spectral density of the thermal noise fluctuations[51] prior to experimentation. Stress-relaxation tests were performed on the central region of a cell using a 6.25 μm/s approach velocity and 60 s relaxation time [Fig. 3(A)]. The cantilever descended towards the cell until a trigger force of 2.5 nN was reached, at which point its displacement was stopped and held at a constant displacement for the stress-relaxation portion of the testing. For most cells, this was equivalent to a 1.3–2.1 μm indentation, which corresponds to less than ~15% of the total cell height for an average cell diameter of 12–15 μm. Probe contact with the cell was indicated by a sharp increase in the cantilever deflection.

The data were analyzed using both elastic and viscoelastic models. The indentation approach curve [Fig. 3(B)] was fit with a modified Hertz equation (Eq. 1) to determine the elastic modulus, $E_{elastic}$. The equilibrium modulus, E_{equil}, was calculated using the same equation and the force measurement after 60 s. Data from the relaxation phase of the test [Fig. 3(C)] were fit with the derived viscoelastic equation (Eq. 10) to determine E_R, τ_σ, and τ_ε. E_0, μ, E_Y, k_1, and k_2 were calculated using Eqs. 11–15, which are described in the following section. The Poisson's ratio, ν, was assumed to be 0.38 based on previous studies[20,21,32].

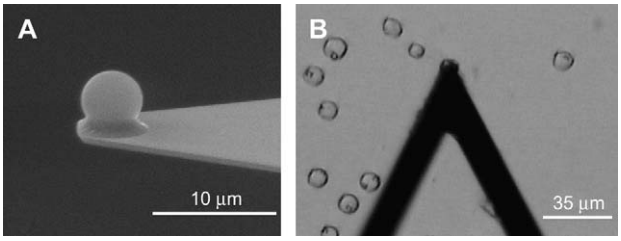

Fig. 2. Single cell indentation using AFM. Individual chondrocytes were tested using a spherical-tipped cantilever (A). Indentation was performed near the center of the cell and any cells that were not round or showed abnormal morphologies were excluded (B). Cell diameters ranged from 7 μm to 15 μm, with the superficial zone chondrocytes being smaller than the middle/deep.

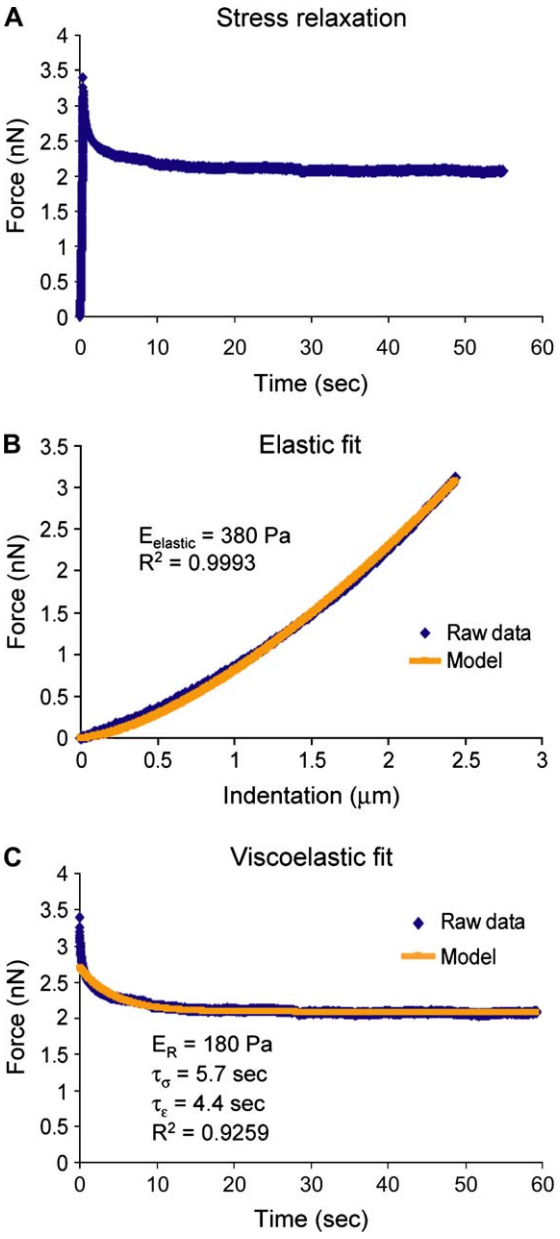

Fig. 3. AFM measurements and curve fitting. Biomechanical testing consisted of rapid indentation of the cell followed by a 60 s stress-relaxation phase (A). The elastic modulus of a cell was extracted from the initial indentation (B). The viscoelastic properties were extracted by fitting the relaxation portion of the curve (C).

STRESS-RELAXATION MODEL FOR AFM

Monitoring the stress-relaxation response to a prescribed displacement is a common method of determining the viscoelastic characteristics of a material. In this AFM-based study, we indented a cell with a step displacement and

recorded the resulting force response over time [Fig. 1(B)]. The force–displacement data were then fitted with an indentation model, which assumes an infinitely hard sphere indenting a flat, deformable substrate, and can be described by a modified Hertz equation[52]:

$$F = \frac{4E_Y R^{1/2}}{3(1-\nu^2)}\delta^{3/2}, \tag{1}$$

where F is the applied force, E_Y is the Young's modulus, R is the relative radius, ν is the Poisson's ratio, and δ is the indentation. The relative radius describes contact between two spheres[53–55], such as the probe tip and a cell, and is defined as:

$$R = \left(\frac{1}{R_{tip}} + \frac{1}{R_{cell}}\right)^{-1}. \tag{2}$$

For this study, $R_{tip} = 2.5$ μm and $R_{cell} = 5.9$ μm (superficial) or 7.05 μm (middle/deep), dimensions that were measured using the micropipette aspiration setup. The modified Hertz equation (Eq. 1), when used with the initial indentation phase of the data, describes the elastic response of a cell [Fig. 1(B)].

Using the Hertz equation and work by Theret *et al.*[24], we derived a viscoelastic solution for small indentations of an isotropic, incompressible surface with a hard, spherical indenter. Variables and constants used in the derivation are defined at the end of this article. To determine the viscoelastic response for this system, the basic elastic (Eq. 3) and viscoelastic (Eq. 4) solutions are first transformed into the Laplace domain [Eqs. 3(a) and 4(a)] and solved for their stress/strain ratios [Eqs. 3(b) and 4(b)]:

$$\sigma = 2G(t)\varepsilon, \tag{3}$$

$$\overline{\sigma} = 2\overline{G}(s)\overline{\varepsilon}, \tag{3a}$$

$$\frac{\overline{\sigma}}{\overline{\varepsilon}} = 2\overline{G}(s), \tag{3b}$$

and

$$\left(1 + \tau_\varepsilon \frac{d}{dt}\right)\sigma = E_R\left(1 + \tau_\sigma \frac{d}{dt}\right)\varepsilon, \tag{4}$$

$$(1 + \tau_\varepsilon s)\overline{\sigma} = E_R(1 + \tau_\sigma s)\overline{\varepsilon}, \tag{4a}$$

$$\frac{\overline{\sigma}}{\overline{\varepsilon}} = \frac{E_R(1 + \tau_\sigma s)}{(1 + \tau_\varepsilon s)}. \tag{4b}$$

Using the correspondence principle, the general elastic [Eq. 3(b)] and viscoelastic [Eq. 4(b)] solutions can be combined in the Laplace domain to obtain an equation describing the modulus of rigidity, G:

$$\overline{G}(s) = \frac{1}{2}\frac{E_R(1 + \tau_\sigma s)}{(1 + \tau_\varepsilon s)}. \tag{5}$$

Since the modulus of rigidity is related to the Young's modulus, E_Y, through:

$$G = \frac{E_Y}{2(1+\nu)}, \tag{6}$$

the Young's modulus can be represented by:

$$\overline{E}(s) = 2(1+\nu)\overline{G}(s) = (1+\nu)\left[\frac{E_R(1 + \tau_\sigma s)}{(1 + \tau_\varepsilon s)}\right]. \tag{7}$$

Under stress-relaxation conditions (constant deformation), the indentation response of Eq. (1) can be approximated by using the Heaviside step function, $H(t)$:

$$F(t) = \frac{4E(t)R^{1/2}}{3(1-\nu^2)}\delta_0^{3/2}H(t). \tag{8}$$

After transforming this equation into the Laplace domain,

$$\overline{F}(s) = \frac{4\overline{E}(s)R^{1/2}}{3(1-\nu^2)}\frac{\delta_0^{3/2}}{s}, \tag{9}$$

and substituting for $\overline{E}(s)$ with Eq. 7,

$$\overline{F}(s) = \frac{4R^{1/2}\delta_0^{3/2}E_R}{3(1-\nu)}\frac{(1 + \tau_\sigma s)}{s(1 + \tau_\varepsilon s)}, \tag{10}$$

the viscoelastic solution can be obtained by transforming the equation back to the time domain:

$$F(t) = \frac{4R^{1/2}\delta_0^{3/2}e_R}{3(1-\nu)}\left(1 + \frac{\tau_\sigma - \tau_\varepsilon}{\tau_\varepsilon}e^{-t/\tau_\varepsilon}\right), \tag{11}$$

where τ_σ and τ_ε are the relaxation times under constant load and deformation, respectively. Fitting Eq. 11 to a force–displacement curve provides three parameters that describe a cell's viscoelastic response as a standard linear solid (a spring-dashpot in parallel with another spring):

$$k_1 = E_R, \tag{12}$$

$$k_2 = E_R\frac{(\tau_\sigma - \tau_\varepsilon)}{\tau_\varepsilon}, \tag{13}$$

and

$$\mu = E_R(\tau_\sigma - \tau_\varepsilon), \tag{14}$$

where k_1 and k_2 are Kelvin spring elements and μ is the apparent viscosity. The instantaneous and Young's moduli can then be calculated as follows:

$$E_0 = E_R\left(1 + \frac{\tau_\sigma - \tau_\varepsilon}{\tau_\varepsilon}\right) \tag{15}$$

and

$$E_Y = \frac{3}{2}E_R. \tag{16}$$

For this study, AFM data were fit to Eqs. 1 and 11 to determine the elastic and viscoelastic properties of single cells.

MICROPIPETTE ASPIRATION

The viscoelastic properties of middle/deep chondrocytes were also measured using micropipette aspiration[21,23] on a separate set of specimens ($N = 5$) to verify the results obtained by AFM (Fig. 4). Briefly, harvested cells were placed in a microscope chamber that allowed side access with a micropipette. The micropipettes and bottom coverslip of the chamber were coated with Sigmacote (Sigma) to prevent cell adhesion. Pressures were applied to the surface of a chondrocyte through the micropipette (5.5 μm diameter) with a custom-built adjustable water reservoir and measured with an in-line pressure transducer having a resolution of 1 Pa (Model no. DP15-28, Validyne Engineering Corp., Northridge, CA). Video images of cell deformation during aspiration were recorded on an S-VHS videotape recorder at 60 fields/s with a CCD camera (COHU, San Diego, CA) through a bright-field microscope (Diaphot 300, Nikon Inc.,

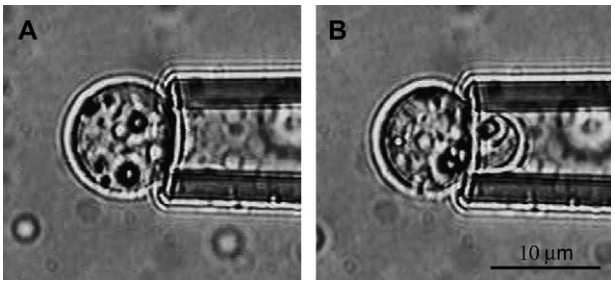

Fig. 4. Micropipette aspiration. Creep response tests were conducted on single chondrocytes in suspension. Zonal cells were equilibrated at a tare pressure (A) before applying a step, negative pressure to induce creep (B). Video measurements of the aspiration length over time were used to determine the viscoelastic properties of the cells.

Melville, NY), using a 60× oil immersion objective (numerical aperture = 1.40) (Nikon) and a 10× wide field eyepiece (Edmund Scientific Co., Barrington, NJ). The applied pressures and time were displayed on a video monitor using a digital multiplexer (Vista Electronics, Ramona, CA) and recorded to videotape. The length of cell aspiration was measured with a video caliper system (resolution ± 0.2 μm). For creep testing of individual chondrocytes, a tare pressure (0.01 kPa) was applied to the cells which were allowed to equilibrate for 60 s. At equilibrium, a step increase in pressure (0.03–0.68 kPa, dependent on cell) was applied and data were collected for 300 s. The aspiration length, time, and applied pressure were recorded for use in determining the cell's viscoelastic properties. The horizontal and vertical diameters of each cell were also measured, and the average of these measurements was reported as the cell diameter.

The viscoelastic properties of the cell were calculated based on an analytical solution of the micropipette aspiration experiment[25]. This model assumes that the cell is a homogeneous, isotropic, linear, viscoelastic, three-parameter, solid half-space and provides a closed form solution for the length of aspiration, L, in terms of the time, t, the applied pressure, Δp, the inner micropipette radius, a, and the wall parameter, Φ (based on the ratio of the thickness to the radius of the micropipette, equal to 2.1 in this case). Previous numerical simulations of the experimental geometry have shown that the measured properties are relatively insensitive to the sizes of the cells and micropipette for most configurations[56,57]. Values for k_1, k_2, and μ were calculated by fitting the experimental data to the following equation[25]:

$$L = \frac{a\Delta p\Phi(\eta)}{\pi k_1}\left[1 - \frac{k_2}{k_1 + k_2}\exp\left(-\frac{k_1 k_2}{(k_1 + k_2)\mu}t\right)\right]. \quad (17)$$

STATISTICAL ANALYSIS

A sample size of $n = 49$ cells for the superficial zone and $n = 72$ cells for the middle/deep zone from eight animals was used for testing zonal chondrocytes with AFM stress-relaxation. An additional five animals were used for comparison tests with micropipette aspiration ($n = 38$ middle/deep cells). Single-factor analysis of variance (ANOVA) was conducted to determine whether significant differences existed, with statistical significance reported at the 95% confidence level ($P < 0.05$), between the biomechanical properties of superficial and middle/deep zone cells and between results for the AFM and micropipette aspiration methods.

Results

AFM

Using the closed-loop control system, a near-step displacement was applied to single cells using the spherical-tipped cantilevers. The 2.5 nN trigger force resulted in an average indentation of 1.65 ± 0.53 μm, which was approximately 15% of the cell height. All cells exhibited stress-relaxation behavior consistent with a viscoelastic solid material, reaching an equilibrium reaction force in approximately 30 s. Excellent agreement between the theoretical model fits and the experimental data for both elastic ($R^2 = 0.994 \pm 0.012$) and viscoelastic ($R^2 = 0.857 \pm 0.081$) models were obtained. Zonal comparisons indicated that superficial cells (S) had significantly higher values for all measured properties, $E_{elastic}$, E_{equil}, E_R, E_0, and μ, when measured with AFM (Table I). Superficial chondrocytes had a 108% higher elastic modulus, 75% higher elastic equilibrium modulus, 82% higher relaxed modulus, 90% higher instantaneous modulus, and 89% higher apparent viscosity than middle/deep chondrocytes ($P < 0.0001$ for all comparisons).

MICROPIPETTE ASPIRATION

In response to a step increase in pressure, chondrocytes exhibited a rapid jump in displacement, followed by creep to equilibrium. The moduli obtained by micropipette aspiration were slightly different than those measured by AFM (Table I). Middle/deep chondrocytes measured by micropipette aspiration showed a 35% lower relaxed modulus ($P < 0.0001$) and 21% higher instantaneous modulus ($P < 0.0001$). The apparent viscosity showed a major difference between the two testing methods, with micropipette aspiration resulting in a 320% higher apparent viscosity measurement than AFM ($P < 0.0001$). A significant difference was also measured between the average diameter of S and M/D (11.8 ± 0.9 μm vs 14.1 ± 1.0 μm, $P < 0.0001$).

Discussion

The findings of this study, aimed at determining the mechanical properties of isolated chondrocytes, suggest that the mechanical properties of chondrocytes from different

Table I
Biomechanical properties of zonal, articular chondrocytes using AFM and verification by micropipette aspiration

	AFM		Micropipette aspiration
	Superficial	Middle/deep	Middle/deep
E_R (Pa)	310 ± 150*	170 ± 90*, #	140 ± 50#
τ_σ (s)	9.6 ± 6.0	9.0 ± 6.2#	37 ± 26#
τ_ε (s)	5.0 ± 2.8	5.2 ± 3.5#	18 ± 15#
k_1 (Pa)	310 ± 150*	170 ± 90*, #	140 ± 50#
k_2 (Pa)	250 ± 120*	120 ± 70*, #	170 ± 70#
$k_1 + k_2$ (Pa)	550 ± 230*	290 ± 140*	300 ± 90
μ (Pa s)	1150 ± 660*	610 ± 690*, #	2570 ± 1830#
E_0 (Pa)	550 ± 230*	290 ± 140*, #	450 ± 140#
E_Y (Pa)	460 ± 220*	260 ± 140*, #	200 ± 70#
$E_{elastic}$ (Pa)	1270 ± 610*	610 ± 340*	–
E_{equil} (Pa)	420 ± 210*	240 ± 130*	–

*Significant difference between zones ($P < 0.05$). #Significant difference between methods ($P < 0.05$).

zones of the tissue differ significantly. Importantly, results obtained using two different micromechanical testing methods, AFM stress-relaxation and micropipette aspiration creep, yielded generally similar values for the mechanical properties. Although micropipette aspiration provides a reliable method for measuring the mechanical properties of cells in suspension, the method may be limited in certain testing configurations, such as for cells in a monolayer. AFM is an attractive option for measuring cell properties in these situations since an indentation can be performed on attached cells using a relatively small tip compression. Given the respective advantages and disadvantages of these techniques, our findings support the utility of both these methods for determining the intrinsic mechanical behavior of single cells.

While the mechanical properties of chondrocytes measured by AFM and micropipette aspiration were on the same order of magnitude, the Young's modulus was 35% lower and the instantaneous modulus was 21% higher when measured by micropipette aspiration. Given the large disparities in such properties reported by other techniques such as cytoindentation and unconfined compression (Table II), our findings suggest that the differences between AFM and micropipette aspiration measurements, while statistically significant, are relatively small. Previous AFM studies of cell mechanics[34–38,40,42,58] typically used pyramidal, AFM probe tips with an approximate radius of curvature of 20–45 nm. In this study, we use a 5 μm diameter sphere as the probe tip to decrease the local strains at the point of contact. Furthermore, since the micropipette diameter is similar to the size of the microsphere, the two methods test a similar area of the cell. Nonetheless, significant differences exist in the testing configurations that must be taken into account in the interpretation of the data. The micropipette aspiration method applies a suction pressure to the cell surface, while AFM indentation applies a compressive force. However, shear deformation is likely the primary deformation mechanism in both techniques[36,59], as chondrocytes have been shown to be fairly incompressible ($\nu \sim 0.4$)[26,60]. Although chondrocytes maintain a spherical shape in both testing configurations, one important difference between the two techniques is the fact that cells are attached to a PLL-coated substrate for AFM experiments, while they are in free suspension for micropipette aspiration. As cell adhesion can induce changes in cytoskeletal structure that arise from various integrin and cell-surface receptor mediated interactions[61], it is possible that the lower apparent viscosity measured by AFM can be attributed to this difference between the two configurations.

An important consideration in the interpretation of this data is the assumption of infinitesimal strain used to determine the stress-relaxation solution. In our study, nominal strains during indentation were 10–15%, suggesting that some error may be introduced into the measured properties by this assumption. However, such second-order effects represent errors of a few percent and would be expected to be similar between the superficial and middle/deep sample groups. Furthermore, subsequent analysis with a thin-layer model[62] that accounts for potential geometric considerations showed that there was typically less than 5% variation between the two models, which indicated that a 15% strain in our case still resulted in properties similar to those measured by micropipette aspiration.

The zonal structure of articular cartilage is often defined by variations in the composition and structure of the tissue as well as differences in cell shape and arrangement with depth from the tissue surface[63]. Although the tissue is typically classified into superficial, middle, and deep zones, previous studies suggest few gene expression and protein synthesis differences between cells of the middle and deep zones, and thus recent studies have examined these groups together. However, several studies have shown significant disparities in the expression of proteins and genes, as well as the overall phenotype, between S and M/D[3–11]. The present study showed that these zonal differences apply to the cells' biomechanical properties as well, with superficial zone cells having significantly higher moduli and apparent viscosities. These findings are consistent with a study that used single cell, unconfined compression to show biomechanical differences existed between zonal chondrocytes[64]. Other recent studies have shown that chondrocyte mechanical properties are primarily dependent on the structure of F-actin in the cell, and that factors associated with altered F-actin organization such as cytochalasin treatment[22], osmotic stress[19], or osteoarthritic disease state[21] influence the apparent viscosity of the cell. These findings are supported by a previous study showing higher actin content in superficial zone chondrocytes in bovine articular cartilage[65]. It is expected that increased F-actin organization would also be reflected in an increased cell modulus, which was also shown by this study's results.

The mechanical microenvironment of the chondrocyte has been shown to depend on the relative properties of the cell, its pericellular matrix and the extracellular matrix[12,13]. While the extracellular matrix shows differences in compressive properties of more than an order of magnitude from the superficial to the deep zones[16–18], micropipette analysis of the pericellular matrix showed no zonal dependency[15,66]. Taken together with the findings of the current study, numerical models of cell–matrix interactions suggest that the relative properties of the pericellular and extracellular matrices will play a more dominant role in defining the biomechanical microenvironment of the chondrocyte. However, previous studies have shown that F-actin may play a role in the

Table II
Comparison of viscoelastic properties for single chondrocytes (middle/deep zone) using AFM, micropipette aspiration, indentation, and unconfined compression

	AFM (current study)*	Micropipette aspiration (current study)*	Micropipette aspiration[21]†	Cytoindentation[31]‡	Unconfined compression[64]‡
E_R (Pa)	170 ± 90	140 ± 50	240 ± 110	1090 ± 400	640 ± 310
E_0 (Pa)	290 ± 140	450 ± 140	410 ± 170	8000 ± 4410	780 ± 380
μ (Pa s)	610 ± 690	2570 ± 1830	3000 ± 1800	1500 ± 920	3180 ± 7330

*Porcine.
†Human.
‡Bovine.

transmission of mechanical signals intracellularly to the nucleus and potentially to other organelles[67]. Thus any zonal differences in cellular properties may still influence intracellular signaling processes that are responsible for the observed zonal dependency of chondrocyte response to mechanical stress[11]. It is also important to note that in addition to matrix structure composition, significant differences may exist in the physicochemical environment of the tissue with depth from the surface. Because the primary nutrient supply for cartilage is through diffusion from the synovial fluid at the tissue surface, it is likely that gradients in oxygen, nutrients, metabolites, pH, osmotic pressure, etc. exist from the superficial to the deep zones, potentially influencing cellular properties and behavior[68–70].

In summary, our findings show that the viscoelastic mechanical properties of isolated chondrocytes can be measured accurately using AFM stress-relaxation. Zonal differences have been reported previously in chondrocyte biosynthetic activity and gene expression, and our findings suggest that chondrocyte biomechanical properties also vary based on the zone of origin. Given the versatility and dynamic testing capabilities of the AFM, the ability to conduct stress-relaxation measurements using this technique may provide further new techniques for studying the viscoelastic properties of cells under a variety of testing configurations.

Acknowledgments

This work was supported in part by NIH grants EB01630, AG15768, AR48182, and AR50245. We would like to thank Frank Moutos and John Tedrow for their assistance in early aspects of this study. We would also like to thank Nehal Abu-Lail for her assistance in the Nanomechanics AFM Laboratory and Asylum Research for their help and guidance in developing the stress-relaxation procedure for the MFP-3D AFM.

Definitions of variables and constants used in this paper

$E_{elastic}$	Elastic modulus (from Hertz model)
E_{equil}	Equilibrium modulus (from Hertz model at equilibrium)
F	Force
δ	Indentation
E_0	Instantaneous modulus
k_1, k_2	Kelvin spring elements
μ	Kelvin viscous element, apparent viscosity
G	Modulus of rigidity
ν	Poisson's ratio
R	Radius of probe tip
E_R	Relaxed modulus
ε	Strain
σ	Stress
τ_σ	Time of relaxation of deformation under constant load
τ_ε	Time of relaxation of load under constant deformation
E_Y	Young's modulus

References

1. Guilak F, Sah RL, Setton LA. Physical regulation of cartilage metabolism. In: Mow VC, Hayes WC, Eds. Basic Orthopaedic Biomechanics. 2nd edn. Philadelphia: Lippincott-Raven 1997:179–207.
2. Shieh AC, Athanasiou KA. Principles of cell mechanics for cartilage tissue engineering. Ann Biomed Eng 2003;31(1):1–11.
3. Aydelotte MB, Kuettner KE. Differences between subpopulations of cultured bovine articular chondrocytes. I. Morphology and cartilage matrix production. Connect Tissue Res 1988;18(3):205–22.
4. Darling EM, Hu JCY, Athanasiou KA. Zonal and topographical differences in articular chondrocyte gene expression. J Orthop Res 2004;22(6):1182–7.
5. Flannery CR, Hughes CE, Schumacher BL, Tudor D, Aydelotte MB, Kuettner KE, *et al*. Articular cartilage superficial zone protein (SZP) is homologous to megakaryocyte stimulating factor precursor and is a multifunctional proteoglycan with potential growth-promoting, cytoprotective, and lubricating properties in cartilage metabolism. Biochem Biophys Res Commun 1999;254(3):535–41.
6. Lorenzo P, Bayliss MT, Heinegard D. A novel cartilage protein (CILP) present in the mid-zone of human articular cartilage increases with age. J Biol Chem 1998; 273(36):23463–8.
7. Archer CW, McDowell J, Bayliss MT, Stephens MD, Bentley G. Phenotypic modulation in sub-populations of human articular chondrocytes *in vitro*. J Cell Sci 1990;97(Pt 2):361–71.
8. Siczkowski M, Watt FM. Subpopulations of chondrocytes from different zones of pig articular cartilage. Isolation, growth and proteoglycan synthesis in culture. J Cell Sci 1990;97(Pt 2):349–60.
9. Zanetti M, Ratcliffe A, Watt FM. Two subpopulations of differentiated chondrocytes identified with a monoclonal antibody to keratan sulfate. J Cell Biol 1985;101(1): 53–9.
10. Aydelotte MB, Greenhill RR, Kuettner KE. Differences between sub-populations of cultured bovine articular chondrocytes. II. Proteoglycan metabolism. Connect Tissue Res 1988;18(3):223–34.
11. Lee DA, Noguchi T, Knight MM, O'Donnell L, Bentley G, Bader DL. Response of chondrocyte subpopulations cultured within unloaded and loaded agarose. J Orthop Res 1998;16(6):726–33.
12. Guilak F, Mow VC. The mechanical environment of the chondrocyte: a biphasic finite element model of cell–matrix interactions in articular cartilage. J Biomech 2000;33(12):1663–73.
13. Alexopoulos LG, Setton LA, Guilak F. The biomechanical role of the chondrocyte pericellular matrix in articular cartilage. Acta Biomater 2005;1(3):317–25.
14. Guilak F, Alexopoulos LG, Haider MA, Ting-Beall HP, Setton LA. Zonal uniformity in mechanical properties of the chondrocyte pericellular matrix: micropipette aspiration of canine chondrons isolated by cartilage homogenization. Ann Biomed Eng 2005;33:1312–8.
15. Alexopoulos LG, Haider MA, Vail TP, Guilak F. Alterations in the mechanical properties of the human chondrocyte pericellular matrix with osteoarthritis. J Biomech Eng 2003;125(3):323–33.
16. Mow VC, Guo XE. Mechano-electrochemical properties of articular cartilage: their inhomogeneities and anisotropies. Annu Rev Biomed Eng 2002;4:175–209.
17. Schinagl RM, Gurskis D, Chen AC, Sah RL. Depth-dependent confined compression modulus of full-thickness bovine articular cartilage. J Orthop Res 1997;15(4):499–506.
18. Wang CC, Chahine NO, Hung CT, Ateshian GA. Optical determination of anisotropic material properties of

bovine articular cartilage in compression. J Biomech 2003;36(3):339–53.
19. Guilak F, Erickson GR, Ping Ting-Beall H. The effects of osmotic stress on the viscoelastic and physical properties of articular chondrocytes. Biophys J 2002; 82:720–7.
20. Jones WR, Ting-Beall HP, Lee GM, Kelley SS, Hochmuth RM, Guilak F. Alterations in the Young's modulus and volumetric properties of chondrocytes isolated from normal and osteoarthritic human cartilage. J Biomech 1999;32(2):119–27.
21. Trickey WR, Lee GM, Guilak F. Viscoelastic properties of chondrocytes from normal and osteoarthritic human cartilage. J Orthop Res 2000;18(6):891–8.
22. Trickey WR, Vail TP, Guilak F. The role of the cytoskeleton in the viscoelastic properties of human articular chondrocytes. J Orthop Res 2004;22(1):131–9.
23. Hochmuth RM. Micropipette aspiration of living cells. J Biomech 2000;33(1):15–22.
24. Theret DP, Levesque MJ, Sato M, Nerem RM, Wheeler LT. The application of a homogeneous half-space model in the analysis of endothelial cell micropipette measurements. J Biomech Eng 1988;110(3):190–9.
25. Sato M, Theret DP, Wheeler LT, Ohshima N, Nerem RM. Application of the micropipette technique to the measurement of cultured porcine aortic endothelial cell viscoelastic properties. J Biomech Eng 1990;112(3):263–8.
26. Freeman PM, Natarjan RN, Kimura JH, Andriacchi TP. Chondrocyte cells respond mechanically to compressive loads. J Orthop Res 1994;12:311–20.
27. Lee DA, Bader DL. The development and characterization of an *in vitro* system to study strain-induced cell deformation in isolated chondrocytes. *In Vitro* Cell Dev Biol Anim 1995;31(11):828–35.
28. McConnaughey WB, Petersen NO. Cell poker: an apparatus for stress–strain measurements on living cells. Rev Sci Instrum 1980;51(5):575–80.
29. Daily B, Elson EL, Zahalak GI. Cell poking. Determination of the elastic area compressibility modulus of the erythrocyte membrane. Biophys J 1984;45(4): 671–82.
30. Duszyk M, Schwab B 3rd, Zahalak GI, Qian H, Elson EL. Cell poking: quantitative analysis of indentation of thick viscoelastic layers. Biophys J 1989;55(4): 683–90.
31. Koay EJ, Shieh AC, Athanasiou KA. Creep indentation of single cells. J Biomech Eng 2003;125(3):334–41.
32. Shin D, Athanasiou K. Cytoindentation for obtaining cell biomechanical properties. J Orthop Res 1999;17(6): 880–90.
33. Leipzig ND, Athanasiou KA. Unconfined creep compression of chondrocytes. J Biomech 2005;38(1):77–85.
34. Hoh JH, Schoenenberger CA. Surface morphology and mechanical properties of MDCK monolayers by atomic force microscopy. J Cell Sci 1994;107(Pt 5):1105–14.
35. Costa KD. Single-cell elastography: probing for disease with the atomic force microscope. Dis Markers 2004; 19:139–54.
36. Costa KD, Yin FC. Analysis of indentation: implications for measuring mechanical properties with atomic force microscopy. J Biomech Eng 1999;121(5):461–71.
37. Vinckier A, Semenza G. Measuring elasticity of biological materials by atomic force microscopy. FEBS Lett 1998;430(1–2):12–6.
38. Shroff SG, Saner DR, Lal R. Dynamic micromechanical properties of cultured rat atrial myocytes measured by atomic force microscopy. Am J Physiol 1995; 269(1 Pt 1):C286–92.
39. Park S, Costa KD, Ateshian GA. Microscale frictional response of bovine articular cartilage from atomic force microscopy. J Biomech 2004;37(11):1679–87.
40. Hu K, Radhakrishnan P, Patel RV, Mao JJ. Regional structural and viscoelastic properties of fibrocartilage upon dynamic nanoindentation of the articular condyle. J Struct Biol 2001;136(1):46–52.
41. Stolz M, Raiteri R, Daniels AU, VanLandingham MR, Baschong W, Aebi U. Dynamic elastic modulus of porcine articular cartilage determined at two different levels of tissue organization by indentation-type atomic force microscopy. Biophys J 2004;86(5):3269–83.
42. Tomkoria S, Patel RV, Mao JJ. Heterogeneous nanomechanical properties of superficial and zonal regions of articular cartilage of the rabbit proximal radius condyle by atomic force microscopy. Med Eng Phys 2004; 26(10):815–22.
43. Ng L, Ortiz C, Grodzinsky AJ. Visualization and nanomechanical properties of individual chondrocytes with an increasingly thick pericellular matrix. Trans Orthop Res Soc 2005. Washington, D.C.: Paper No: 0182.
44. Bader DL, Ohashi T, Knight MM, Lee DA, Sato M. Deformation properties of articular chondrocytes: a critique of three separate techniques. Biorheology 2002;39(1–2):69–78.
45. Hung CT, Costa KD, Guo XE. Apparent and transient mechanical properties of chondrocytes during osmotic loading using triphasic theory and AFM indentation. ASME Bioengineering Conference 2001.
46. Radmacher M, Fritz M, Kacher CM, Cleveland JP, Hansma PK. Measuring the viscoelastic properties of human platelets with the atomic force microscope. Biophys J 1996;70(1):556–67.
47. Mahaffy RE, Park S, Gerde E, Kas J, Shih CK. Quantitative analysis of the viscoelastic properties of thin regions of fibroblasts using atomic force microscopy. Biophys J 2004;86(3):1777–93.
48. Mahaffy RE, Shih CK, MacKintosh FC, Kas J. Scanning probe-based frequency-dependent microrheology of polymer gels and biological cells. Phys Rev Lett 2000;85(4):880–3.
49. Fung YC. Biomechanics: its scope, history, and some problems of continuum mechanics in physiology. Appl Mech Rev 1968;21:1–20.
50. Kuettner KE, Pauli BU, Gall G, Memoli VA, Schenk RK. Synthesis of cartilage matrix by mammalian chondrocytes *in vitro*. I. Isolation, culture characteristics, and morphology. J Cell Biol 1982;93(3):743–50.
51. Hutter JL, Bechhoefer J. Calibration of atomic-force microscope tips. Rev Sci Instrum 1993;64:1868–73.
52. Harding JW, Sneddon IN. The elastic stresses produced by the indentation of the plane surface of a semi-infinite elastic solid by a rigid punch. Proc Cambridge Philos Soc 1945;41:16–26.
53. Lu WM, Tung KL, Hung SM, Shiau JS, Hwang KJ. Compression of deformable gel particles. Powder Technology 2001;116(1):1–12.
54. Lin YY, Hui CY. Mechanics of contact and adhesion between viscoelastic spheres: an analysis of hysteresis during loading and unloading. J Polym Sci Part B-Polymer Physics 2002;40(9):772–93.
55. Johnson KL. Contact Mechanics. Cambridge, United Kingdom: Cambridge University Press 1985.
56. Haider MA, Guilak F. An axisymmetric boundary integral model for assessing elastic cell properties in the

micropipette aspiration contact problem. J Biomech Eng 2002;124(5):586–95.
57. Baaijens FP, Trickey WR, Laursen TA, Guilak F. Large deformation finite element analysis of micropipette aspiration to determine the mechanical properties of the chondrocyte. Ann Biomed Eng 2005;33(4):494–501.
58. Allen DM, Mao JJ. Heterogeneous nanostructural and nanoelastic properties of pericellular and interterritorial matrices of chondrocytes by atomic force microscopy. J Struct Biol 2004;145(3):196–204.
59. Baaijens FP, Trickey WR, Laursen TA, Guilak F. Large deformation finite element analysis of micropipette aspiration to determine the mechanical properties of the chondrocyte. Ann Biomed Eng 2005;33:494–501.
60. Trickey WR, Baaijens FP, Laursen TA, Alexopoulos LG, Guilak F. Determination of the Poisson's ratio of the cell: recovery properties of chondrocytes after release from complete micropipette aspiration. J. Biomech 2006;39:78–87.
61. Knudson W, Loeser RF. CD44 and integrin matrix receptors participate in cartilage homeostasis. Cell Mol Life Sci 2002;59(1):36–44.
62. Dimitriadis EK, Horkay F, Maresca J, Kachar B, Chadwick RS. Determination of elastic moduli of thin layers of soft material using the atomic force microscope. Biophys J 2002;82(5):2798–810.
63. Eggli PS, Hunziker EB, Schenk RK. Quantitation of structural features characterizing weight- and less-weight-bearing regions in articular cartilage: a stereological analysis of medial femoral condyles in young adult rabbits. Anat Rec 1988;222(3):217–27.
64. Shieh AC, Athanasiou KA. Biomechanics of single zonal chondrocytes. J Biomech 2006 (in press). doi:10.1016/j.jbiomech.2005.05.002.
65. Langelier E, Suetterlin R, Hoemann CD, Aebi U, Buschmann MD. The chondrocyte cytoskeleton in mature articular cartilage: structure and distribution of actin, tubulin, and vimentin filaments. J Histochem Cytochem 2000;48(10):1307–20.
66. Alexopoulos LG, Williams GM, Upton ML, Setton LA, Guilak F. Osteoarthritic changes in the biphasic mechanical properties of the chondrocyte pericellular matrix in articular cartilage. J Biomech 2005;38(3):509–17.
67. Guilak F. Compression-induced changes in the shape and volume of the chondrocyte nucleus. J Biomech 1995;28(12):1529–41.
68. Zhou S, Cui Z, Urban JP. Factors influencing the oxygen concentration gradient from the synovial surface of articular cartilage to the cartilage–bone interface: a modeling study. Arthritis Rheum 2004;50(12):3915–24.
69. Silver IA. Measurement of pH and ionic composition of pericellular sites. Philos Trans R Soc Lond 1975; 271(912):261–72.
70. Zheng YP, Shi J, Qin L, Patil SG, Mow VC, Zhou KY. Dynamic depth-dependent osmotic swelling and solute diffusion in articular cartilage monitored using real-time ultrasound. Ultrasound Med Biol 2004; 30(6):841–9.